

Phonon-limited inversion layer electron mobility in extremely thin Si layer of silicon-on-insulator metal-oxide-semiconductor field-effect transistor

Masanari Shoji^{a)} and Seiji Horiguchi

NTT Basic Research Laboratories, 3-1, Morinosato Wakamiya, Atsugi-shi, Kanagawa 243-01, Japan

(Received 6 May 1997; accepted for publication 15 September 1997)

Phonon-limited inversion layer electron mobility in extremely thin (100) Si layers of silicon-on-insulator field-effect transistors has been studied at 300 K using a relaxation time approximation and a one-dimensional self-consistent calculation. For the Si layer thickness t_{Si} of more than approximately 5 nm, the mobility behavior as a function of an effective vertical electric field is found to be almost identical with that of bulk Si inversion layers. For a thickness of less than that, however, the mobility behavior is considerably affected by the change in the electronic structures due to a confinement effect. As the Si layer thickness decreases, the phonon-limited electron mobility μ_{ph} increases to a maximum at t_{Si} of ~ 3 nm and decreases monotonically. The increase in mobility results from the increase of the fraction of electrons in the lowest energy subband that has a higher mobility than other subbands. The mobility decrease in the extremely thin t_{Si} region is attributed to the enhancement of phonon scattering rates caused by a reduction of the spatial widths of the subbands. © 1997 American Institute of Physics. [S0021-8979(97)04924-4]

I. INTRODUCTION

Fully depleted silicon-on-insulator (SOI) metal-oxide-semiconductor field-effect transistors (MOSFETs) have a lot of advantages over bulk MOSFETs.¹ The effective carrier mobility μ_{eff} is one of the most significant and essential properties for understanding various transport phenomena and has been studied also in SOI systems.²⁻⁵

Recent articles^{6,7} have clearly given the physical basis of the fundamental mobility behaviors in fully depleted SOI inversion layers by means of an analysis of the electronic structures (potential profile, subband structure, and electron density distribution) of the inversion regions. It has been shown that as long as the Si layer thickness t_{Si} is larger than the inversion layer thickness and the electron density is much higher than the impurity concentration in the inversion region, the electronic structures of an SOI Si inversion region are equivalent to those of a certain bulk Si inversion region. By means of this analysis it has been proved that the mobility behavior of SOI inversion layers as a function of an effective electric field E_{eff} , defined appropriately, is identical with that of bulk Si inversion layers (universal curve⁸⁻¹⁰), irrespective of structural parameters or back gate voltages. On the other hand, it has also been shown that for t_{Si} of less than 10–20 nm, the electronic structures of SOI Si inversion regions are essentially different from those of bulk Si inversion regions, which suggests a distinct mobility behavior in such thin SOI Si inversion layers. For such thin SOI systems, however, there have been no theoretical studies of evaluating μ_{eff} and the experimental results^{4,5} are insufficient for understanding various scattering mechanisms.

In this article, phonon-limited electron mobility of (100) Si inversion layers in such extremely thin SOI systems has

been studied at 300 K using a relaxation time approximation with the results of one-dimensional self-consistent calculations. It is generally accepted that the electron mobility in Si inversion layers is determined by Coulomb scattering, surface roughness scattering, and phonon scattering. Here, only electron-phonon scattering is taken into account as a first step in the analysis of extremely thin SOI systems because electron-phonon interaction is a dominant factor of the mobility in SOI systems without interface roughnesses and interface charges at room temperature. Section II gives an outline of the self-consistent calculation for the electronic structures and some fundamental features of the subband structures. In Sec. III we show the calculated phonon-limited mobility behavior and describe the effects of the extremely thin t_{Si} on this mobility.

II. ELECTRONIC STRUCTURES

One-dimensional calculations of the electronic structures in inversion regions have been performed by solving the Schrödinger and Poisson's equations self-consistently.¹¹ The electronic structures (subband bottom energies, the envelope function in each subband, and the Fermi energy) are required to calculate the mobility in the next section. All calculations were carried out on Si (100) at 300 K with a back gate voltage of 0 V, taking the lowest one hundred subbands into account. Impurity concentrations (N_A) in SOI layer and Si substrate are taken to be $1 \times 10^{15} \text{ cm}^{-3}$ and the buried oxide thickness is 100 nm. We used the longitudinal effective mass m_l of $0.98m_e$ and the transverse effective mass m_t of $0.19m_e$ in Si and the effective mass of $0.5m_e$ in SiO_2 , where m_e is the electron rest mass. The barrier height of SiO_2 for the Si conduction band edge is 3.1 eV and the dielectric constants are 11.9 in Si and 3.9 in SiO_2 . For the envelope function at Si/ SiO_2 interfaces, we have assumed the connection rules that both the envelope function and its derivative divided by the effective mass are continuous. The conduction band of

^{a)}Present address: NTT Integrated Information & Energy Systems Laboratories, 3-9-11, Midori-cho Musashino-shi Tokyo 180 Japan; Electronic mail: mshoji@ilab.ntt.co.jp

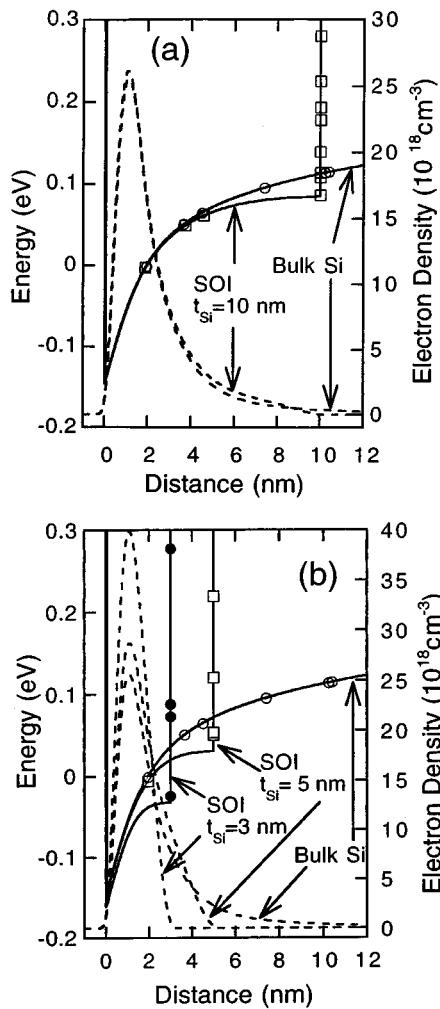


FIG. 1. Potentials, subband bottom energies, and electron density distributions of SOI Si and bulk Si inversion regions at E_{eff} of $5 \times 10^5 \text{ V cm}^{-1}$. Solid and broken lines indicate potential profiles and electron density distributions. The Fermi energy is taken to be 0 eV. Open squares and open circles denote the subband bottom energies of an SOI Si inversion region with t_{Si} of 10 nm and bulk Si inversion region, respectively in (a). Full circles, open squares, and open circles denote subband bottom energies of an SOI Si inversion region with t_{Si} of 3 nm, of 5 nm, and bulk Si inversion region, respectively in (b).

bulk Si has six equivalent valleys along the $\langle 100 \rangle$ directions of the Brillouin zone. In (100) Si inversion layers, there are two series of subbands arising from two different effective masses (m_l and m_t) of the valleys in the direction perpendicular to the surface. The valleys with the heavier effective mass m_l normal to the surface have the degeneracy of two and yield the lowest energy subband. The valleys with the lighter effective mass m_t have the degeneracy of four. We label the heavier effective mass subbands with indices 0, 1, 2, ... and the lighter effective mass subbands with $0', 1', 2', \dots$, as usual.

Figures 1(a) and 1(b) show some results of the self-consistent calculation with N_A of $1 \times 10^{15} \text{ cm}^{-3}$ at E_{eff} of $5 \times 10^5 \text{ V cm}^{-1}$. Figure 1(a) presents the electronic structures of the bulk Si inversion region and the SOI Si inversion region with t_{Si} of 10 nm. The Fermi energy is taken to be 0 eV. For these electronic structures of SOI and bulk Si inversion regions, the potential profiles in the inversion regions

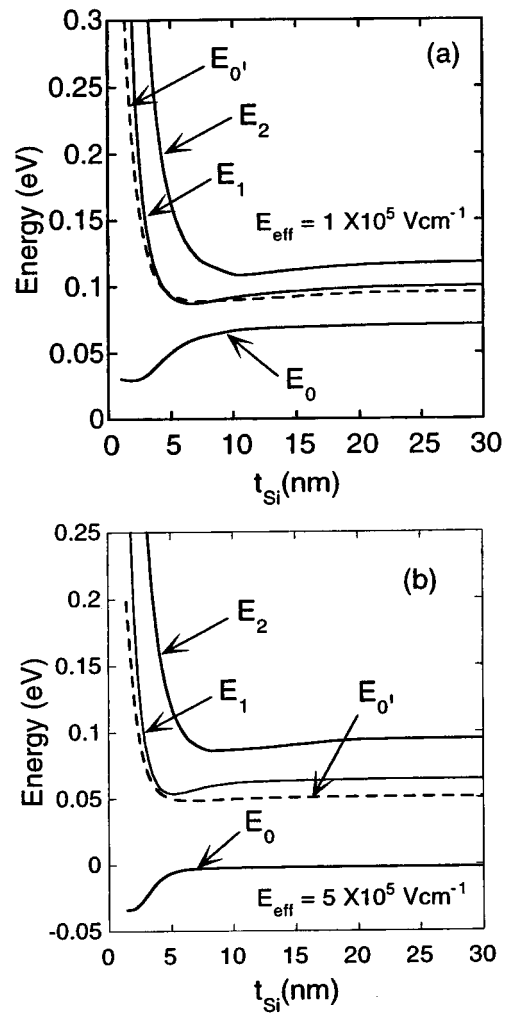


FIG. 2. Bottom energies of the lowest four subbands (0, 1, 2, and $0'$) as a function of Si layer thickness t_{Si} at E_{eff} of $1 \times 10^5 \text{ V cm}^{-1}$ (a) and at E_{eff} of $5 \times 10^5 \text{ V cm}^{-1}$ (b). The energies are measured from the Fermi energy.

are almost the same, the lowest three subband bottom energies (open squares and open circles) are equal and the electron density distributions are identical, which implies that these inversion layers have the same physical properties, including the mobility governed by these electronic structures. (It should be noted that the electronic structures of SOI and bulk Si inversion regions with the same N_A are identical only for low N_A or high E_{eff} .⁶⁾ On the other hand, Fig. 1(b) illustrates the results for the bulk Si inversion region and SOI Si inversion regions with t_{Si} 's of 3 and 5 nm. The electronic structures of these SOI Si inversion regions apparently differ from those of the bulk Si inversion region, which suggests that they have different physical properties from those in the bulk Si inversion layer. Figures 2(a) and 2(b) show the lowest four subband bottom energies in SOI Si inversion regions at $E_{\text{eff}} = 1 \times 10^5$ and $5 \times 10^5 \text{ V cm}^{-1}$ as a function of t_{Si} . In the extremely thin t_{Si} regions, as a consequence of confinement, the energy separations of higher subbands from the lowest subband increase with decreasing t_{Si} . The

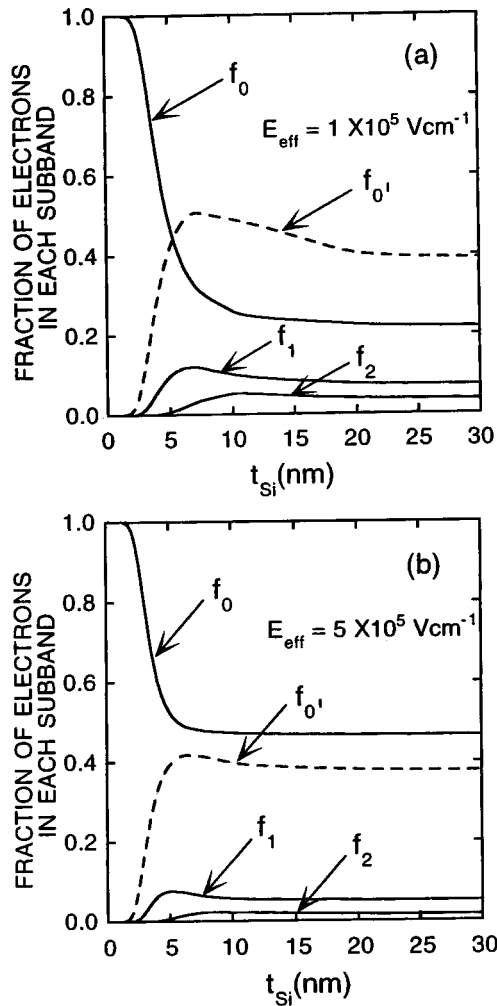


FIG. 3. Fractions of electrons in the lowest four subbands (0, 1, 2, and 0') as a function of Si layer thickness t_{Si} at E_{eff} of $1 \times 10^5 \text{ V cm}^{-1}$ (a) and at E_{eff} of $5 \times 10^5 \text{ V cm}^{-1}$ (b).

corresponding electron population in each subband is shown in Figs. 3(a) and 3(b). It can be seen from Fig. 3 that, as a result of the increase of the energy separations for thin t_{Si} , the electron population in the lowest subband grows rapidly and those in higher subbands decrease with the reduction of t_{Si} . At a lower E_{eff} [Fig. 3(a)], except extremely thin t_{Si} , the fraction of electrons in the 0 subband (f_0) having the lowest bottom energy is lower than that in the 0' subband ($f_{0'}$). This is because the density states mass of the valleys giving the 0' subband is more than twice as heavy as that of the valleys giving the 0 subband and the degeneracy of the former valleys is twice as large as that of the latter valleys. At a higher E_{eff} [Fig. 3(b)], however, f_0 is always higher than $f_{0'}$. This is ascribed to the larger energy separation between E_0 and $E_{0'}$ [Fig. 2(b)] caused by a stronger confinement potential due to a higher electron density.

III. PHONON-LIMITED ELECTRON MOBILITY

Phonon-limited electron mobility of the Si inversion layer in extremely thin SOI structures is calculated using a relaxation time approximation with the results of the self-consistent calculation shown in the previous section. The

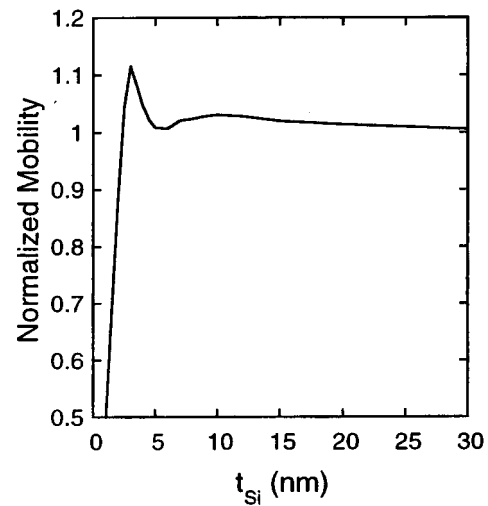


FIG. 4. Calculated phonon-limited electron mobility at E_{eff} of $1 \times 10^5 \text{ V cm}^{-1}$ as a function of the Si layer thickness t_{Si} . The mobility is normalized by the bulk Si inversion layer mobility calculated at the same E_{eff} .

scattering rate of electrons has been evaluated in a conventional procedure¹²⁻¹⁵ employing intravalley acoustic-phonon scattering and intervalley phonon scattering with three g type and three f type intervalley phonons¹⁶ in bulk Si. We have taken account of the subbands having the bottom energies up to more than $10k_B T$ measured from the Fermi energy (k_B is Boltzman constant and T denotes temperature).

Figure 4 shows the phonon-limited mobility at E_{eff} of $1 \times 10^5 \text{ V cm}^{-1}$ as a function of the Si layer thickness t_{Si} . The mobility is normalized by the bulk Si inversion layer mobility calculated at the same E_{eff} . The mobility is almost equal to that of bulk Si inversion layers for t_{Si} of more than approximately 5 nm though a slight enhancement of mobility can be seen around t_{Si} of 10 nm. For the thickness of less than 5 nm, however, the mobility exhibits a significant modification. As the Si layer thickness t_{Si} diminishes, the mobility μ_{ph} increases to more than 10% greater than that of bulk Si inversion layer at t_{Si} of ~ 3 nm and decreases rapidly. Here, we examine the causes of this increase and decrease of μ_{ph} . Figure 5 shows the mobilities of the lowest four subbands (0, 1, 2, and 0') as a function of t_{Si} . It can be seen from Fig. 5 that the lowest subband mobility μ_0 is always higher than other subband mobilities and, for extremely thin t_{Si} , all subband mobilities decrease monotonically with diminishing t_{Si} . One reason for the higher mobility in the lowest subband is that the conductivity effective mass of the valleys from which the lowest subband arises is lighter than that of other valleys. Another reason is that, since final states into which an electron in an initial state scatters must have the same energy as that in the initial state (in the case of intravalley scattering) or the specific energy differences corresponding to intervalley phonon energies (in the case of intervalley scattering), the states into which electrons in the lowest subband can scatter are relatively limited compared with those into which electrons in other higher subbands can scatter. As shown in Fig. 3(a), for t_{Si} of less than ~ 7 nm, the

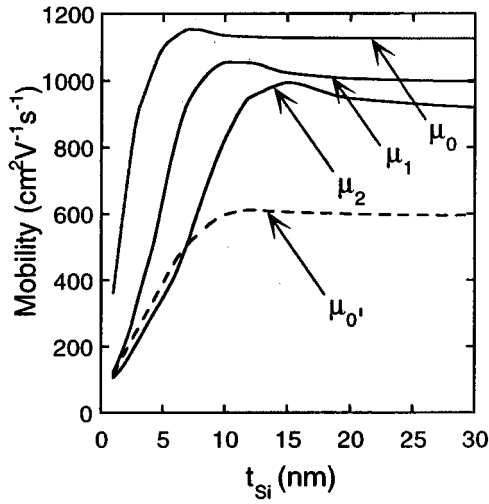


FIG. 5. Electron mobilities of the lowest four subbands (0, 1, 2, and 0') at E_{eff} of $1 \times 10^5 \text{ V cm}^{-1}$ as a function of t_{Si} .

fraction of electrons in the lowest subband (0) rises rapidly and the fractions of electrons in higher subbands (1, 2, and 0') decrease monotonically with the reduction of t_{Si} . These figures [Figs. 3(a) and 5] clearly indicate the reason of the increase of the total mobility μ_{ph} for $t_{\text{Si}}=5-3 \text{ nm}$. Since the total mobility is determined by averaging subband mobilities (μ_i , the lowest four subband mobilities are shown in Fig. 5) weighted by their fractions of electrons [f_i , the fractions for the lowest four subbands are shown in Fig. 3(a)],

$$\mu_{\text{ph}} = \sum_i f_i \mu_i, \quad (1)$$

the increase of μ_{ph} is attributed to the rapid increase of the fraction of electrons in the lowest subband (0) having a higher mobility than other subbands. Namely, the rapid increase of the fraction exceeds the effect of the reduction in each subband mobility for $t_{\text{Si}}=5-3 \text{ nm}$. On the other hand, for t_{Si} of less than $\sim 3 \text{ nm}$ it is obvious that the reduction of the subband mobilities is responsible for the decrease of the total mobility μ_{ph} . This reduction in the subband mobilities is due to an enhancement of the scattering rate caused by an increase in the form factor. Such an enhancement of the scattering rate has been shown for a simple square-well potential with infinitely high walls.^{12,13} The form factor F_{ij} is defined by

$$F_{ij} = \int \zeta_i(z)^2 \zeta_j(z)^2 dz, \quad (2)$$

where z is the coordinate normal to the SiO_2/Si interfaces and $\zeta_i(z)$ is the wave (envelope) function of the i th subband. The scattering rates of both intravalley and intervalley phonon scatterings between the i th and the j th subbands are proportional to F_{ij} .^{12,14,15} It is easy to show that F_{ii} is inversely proportional to the spatial extent of $\zeta_i(z)^2$ or the width of the i th subband $t_{\text{sub},i}$

$$F_{ii} \propto \frac{1}{t_{\text{sub},i}}. \quad (3)$$

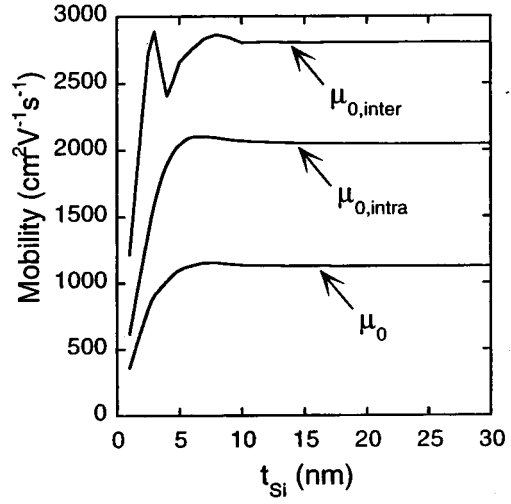


FIG. 6. The lowest subband (0) mobilities limited by intravalley scattering $\mu_{0,\text{intra}}$, by intervalley scattering $\mu_{0,\text{inter}}$, and by both scatterings μ_0 as a function of t_{Si} at E_{eff} of $1 \times 10^5 \text{ V cm}^{-1}$.

In the case of extremely thin t_{Si} , even the widths of the low energy subbands occupied by the inversion electrons are restricted by t_{Si} . In fact, as shown in Fig. 1(b), for $t_{\text{Si}} < \sim 3 \text{ nm}$ even the width of the lowest subband is limited by t_{Si} . Hence, for thin t_{Si}

$$F_{ii} \propto \frac{1}{t_{\text{Si}}}. \quad (4)$$

For such t_{Si} the form factor between different subbands $F_{ij} (i \neq j)$ will also swell with the reduction of t_{Si} . Therefore, for extremely thin t_{Si} , the scattering rate of every subband increases with diminishing t_{Si} . As a result, the mobility μ_{ph} decreases with the reduction of t_{Si} . Since, as shown in Fig. 2, the subband splittings of higher subbands from the lowest subband are larger than a few times $k_B T$ or intervalley phonon energies¹⁶ for extremely thin t_{Si} , the terms containing the form factor F_{00} in the scattering rates (namely, both the intravalley and intervalley scatterings within the equivalent "0" subbands) are dominant in the decrease of μ_{ph} .

Figure 6 shows the lowest subband (0) mobilities limited by intravalley scattering $\mu_{0,\text{intra}}$, by intervalley scattering $\mu_{0,\text{inter}}$, and by both scatterings μ_0 as a function of t_{Si} at E_{eff} of $1 \times 10^5 \text{ V cm}^{-1}$. A suppression of intervalley phonon scatterings can be found around t_{Si} of 3 nm. This suppression is probably ascribed to an enlargement of subband splittings shown in Fig. 2(a). However, intravalley phonon scattering is more dominant and such suppression is insignificant in the total subband mobility μ_0 .

Figure 7 shows the phonon-limited mobility at higher E_{eff} 's of $2 \times 10^5 \text{ V cm}^{-1}$ and $5 \times 10^5 \text{ V cm}^{-1}$ as a function of t_{Si} . The mobility is normalized by the bulk Si inversion layer mobility calculated at each E_{eff} . For t_{Si} of less than 5 nm, with the reduction of t_{Si} , the mobility μ_{ph} increases to a maximum at t_{Si} of $\sim 3 \text{ nm}$ and decreases rapidly, which is qualitatively the same as at E_{eff} of $1 \times 10^5 \text{ V cm}^{-1}$ (Fig. 4). However, the rate of the enhancement at the peak becomes smaller with the increase in E_{eff} . This dependence of the

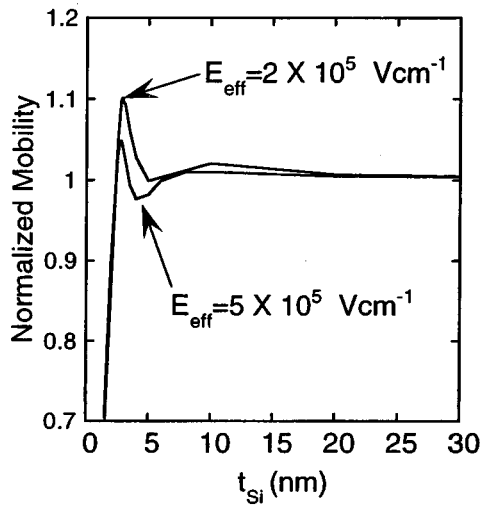


FIG. 7. The phonon-limited electron mobility at E_{eff} 's of $2 \times 10^5 \text{ V cm}^{-1}$ and $5 \times 10^5 \text{ V cm}^{-1}$ as a function of t_{Si} . The mobility is normalized by the bulk Si inversion layer mobility calculated at each E_{eff} .

enhancement rate on E_{eff} can be understood by a property of the electronic structures. As shown in Fig. 3, for thick t_{Si} , the fraction of electrons in the lowest subband (f_0) at higher E_{eff} [Fig. 3(b)] is larger than that at lower E_{eff} [Fig. 3(a)]. Since the increase of μ_{ph} for $t_{\text{Si}}=5-3 \text{ nm}$ is caused by an enlargement of the fraction of electrons in the lowest subband (0), the enhancement rate of μ_{ph} is suppressed at higher E_{eff} .

Recently, it has been suggested that the interaction between inversion electrons and intervalley phonons will be stronger than that in a conventional treatment.¹⁷ In fact, the mobilities produced by our simulation are higher than those of experimental results for bulk Si inversion layers especially in a high E_{eff} region. A higher coupling of electrons and intervalley phonons will make the suppression of intervalley phonon scatterings for thin t_{Si} salient, which will enhance the normalized mobility in an extremely thin t_{Si} range. In order to examine these effects, we have evaluated the mobility using 1.5 times larger deformation potentials for intervalley phonon scatterings. This simulation quantitatively yields the same mobility as that obtained experimentally around an E_{eff} of $5 \times 10^5 \text{ V cm}^{-1}$. Figure 8 shows the results at E_{eff} 's of $1 \times 10^5 \text{ V cm}^{-1}$ and $5 \times 10^5 \text{ V cm}^{-1}$. The mobility is normalized by bulk Si inversion layer mobility determined with the larger deformation potentials at each E_{eff} . For E_{eff} of $1 \times 10^5 \text{ V cm}^{-1}$, the mobility increases up to more than 23% higher than that of the bulk Si inversion layer and the amount of the increase in ratio is more than twice as large as that in the calculation using conventional deformation potentials (Fig. 4). For E_{eff} of $5 \times 10^5 \text{ V cm}^{-1}$, the enhancement rate is also larger than that for conventional deformation potentials. Figure 9 shows the lowest subband (0) mobilities limited by intravalley scattering $\mu_{0,\text{intra}}$, by intervalley scattering $\mu_{0,\text{inter}}$, and by both scatterings μ_0 as a function of t_{Si} at E_{eff} of $1 \times 10^5 \text{ V cm}^{-1}$ when the larger deformation potentials are employed. Since the change of the intervalley deformation potentials influences only the intervalley scattering rates,

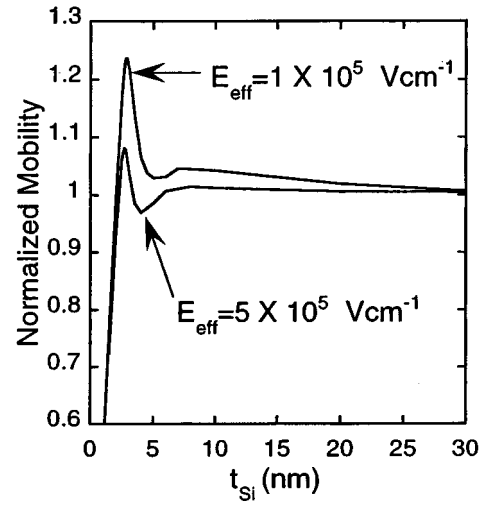


FIG. 8. The phonon-limited electron mobility at E_{eff} 's of $1 \times 10^5 \text{ V cm}^{-1}$ and $5 \times 10^5 \text{ V cm}^{-1}$ as a function of t_{Si} when 1.5 times larger deformation potentials for intervalley phonon scatterings are used. The mobility is normalized by the bulk Si inversion layer mobility calculated with the larger deformation potentials at each E_{eff} .

$\mu_{0,\text{intra}}$ is the same in Figs. 6 and 9. As can be seen from Fig. 9, the intervalley scatterings is dominant ($\mu_{0,\text{intra}} > \mu_{0,\text{inter}}$) as a result of the higher couplings, which makes the effect of the suppression of intervalley scatterings at t_{Si} of $\sim 3 \text{ nm}$ on μ_0 more significant. In consequence, the enhanced rates increase as shown in Fig. 8.

Finally, we mention the quantitative precision in our results for the mobility. For two reasons, the results should be semiquantitative ones. First, the procedure we have employed to obtain the mobility does not quantitatively reproduce the mobility obtained experimentally, even for the bulk Si inversion layers, as well as the procedures in Refs. 17 and 18. This means that further investigations are required to

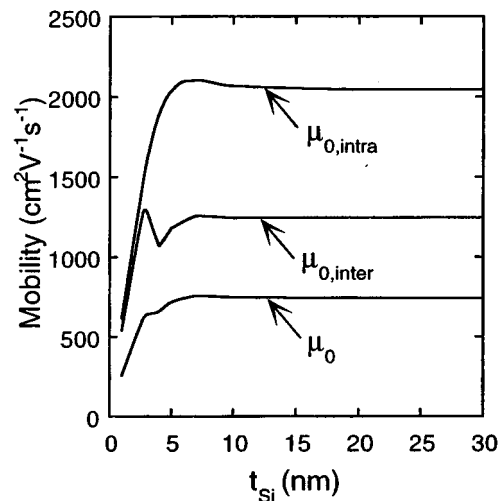


FIG. 9. The lowest subband (0) mobilities limited by intravalley scattering $\mu_{0,\text{intra}}$, by intervalley scattering $\mu_{0,\text{inter}}$, and by both scatterings μ_0 as a function of t_{Si} at E_{eff} of $1 \times 10^5 \text{ V cm}^{-1}$ when using 1.5 times larger deformation potentials for intervalley phonon scatterings.

evaluate the mobility quantitatively. Second, the procedure does not consider the nature of phonons in a thin Si layer sandwiched by SiO₂ but has assumed the nature of phonons in bulk Si for the electron-phonon interactions. The results of the mobility will change quantitatively if the properties of the phonons in such thin SOI systems are taken into account. However, we expect that the results will be semiquantitatively valid. Since it is natural to assume that SiO₂ has low-energy acoustic phonons, thin SOI systems will also have such phonon modes like bulk Si. Consequently, such acoustic phonons cause intravalley phonon scatterings as well, which will also bring about the decrease of μ_{ph} for extremely thin t_{Si} . For other phonons (intervalley phonons), the modification of the mobility is not obvious. However, if the phonons are reduced by, for instance, the quantization in the Si layer,¹⁹ some intervalley phonon scatterings will be suppressed, which leads to a further increase of μ_{ph} for thin t_{Si} . As a result, we expect that the semiquantitative feature (the increase and the decrease of μ_{ph} in extremely thin Si layers) will hold even when taking account of the strict nature of the phonons in thin SOI systems.

IV. SUMMARY

Phonon-limited electron mobility in extremely thin (100) Si layers of SOI MOSFETs has been studied at 300 K using a relaxation time approximation with the results of one-dimensional self-consistent calculations. We have assumed the interaction between electrons and bulk Si phonons. For t_{Si} of more than ~ 5 nm, the mobility behavior of SOI inversion layers as a function of E_{eff} is almost identical with that of bulk Si inversion layers. For t_{Si} of less than that, it has been found that the mobility is considerably affected by two effects, the enhanced fraction of electrons in the lowest subband and the restriction of the spatial extent of each subbands normal to the surface. The former effect contributes to the increase of the mobility μ_{ph} because the lowest subband generally has a high subband mobility compared with other subbands. The latter effect reduces the μ_{ph} by means of the enlargement of the form factor determining the scat-

tering rate. As a result of these effects, the phonon-limited electron mobility increases to a maximum at t_{Si} of ~ 3 nm and decreases monotonically with the reduction of t_{Si} . However, our results are semiquantitative and further investigations of the electron-phonon interactions and the electronic structures are required in order to evaluate the mobility μ_{ph} quantitatively.

ACKNOWLEDGMENT

The authors would like to thank Dr. M. Tomizawa for providing a prototype program for the self-consistent calculation.

- ¹J.-P. Colinge, *Silicon-on-Insulator Technology: Material to VLSI* (Kluwer, Dordrecht, 1991).
- ²M. J. Sherony, L. T. Su, J. E. Chung, and D. A. Antoniadis, *IEEE Trans. Electron Devices* **41**, 276 (1994).
- ³J. Wang, N. Kistler, J. Woo, and C. R. Viswanathan, *IEEE Electron Device Lett.* **15**, 117 (1994).
- ⁴J. Choi, Y. Park, and H. Min, *IEEE Electron Device Lett.* **16**, 527 (1995).
- ⁵A. Toriumi, J. Koga, H. Satake, and A. Ohata, *IEEE IEDM Technical Digest*, 1995, p. 847.
- ⁶M. Shoji, Y. Omura, and M. Tomizawa, *J. Appl. Phys.* **81**, 786 (1997).
- ⁷M. Shoji, Y. Omura, and M. Tomizawa, *Proceedings of Institute of Electrical and Electronics Engineers International Silicon-on-Insulator Conference*, 1995, p. 108.
- ⁸A. E. Sabnis and J. T. Clemens, *IEEE IEDM Technical Digest*, 1979, p. 21.
- ⁹S. Takagi, A. Toriumi, M. Iwase, and H. Tango, *IEEE Trans. Electron Devices* **41**, 2357 (1994).
- ¹⁰S. Takagi, A. Toriumi, M. Iwase, and H. Tango, *IEEE Trans. Electron Devices* **41**, 2363 (1994).
- ¹¹F. Stern, *Phys. Rev. B* **5**, 4891 (1972).
- ¹²P. J. Price, *Ann. Phys. (N.Y.)* **133**, 217 (1981).
- ¹³B. K. Ridley, *J. Phys. C* **15**, 5899 (1982).
- ¹⁴K. Masaki, C. Hamaguchi, K. Taniguchi, and M. Iwase, *Jpn. J. Appl. Phys., Part 1* **28**, 1856 (1989).
- ¹⁵S. Yamakawa, H. Ueno, K. Taniguchi, C. Hamaguchi, K. Miyatsuji, K. Masaki, and U. Ravaioli, *J. Appl. Phys.* **79**, 911 (1996).
- ¹⁶C. Jacoboni and L. Reggiani, *Rev. Mod. Phys.* **55**, 645 (1983).
- ¹⁷S. Takagi, J. L. Hoyt, J. J. Welser, and J. F. Gibbons, *J. Appl. Phys.* **80**, 1567 (1996).
- ¹⁸M. V. Fischetti and S. E. Laux, *Phys. Rev. B* **48**, 2244 (1993).
- ¹⁹P. Butcher, N. H. March, and M. P. Tosi, *Physics of Low-Dimensional Semiconductor Structures* (Plenum, New York, 1993).